JOC Article
pubs.acs.org/joc

Effect of Electron-Withdrawing Substituents on the Epoxide Ring: An Experimental and Theoretical Electron Density Analysis of a Series of Epoxide Derivatives

Simon Grabowsky,*[,†] Tanja Schirmeister,[‡] Carsten Paulmann,[§] Thomas Pfeuffer,[‡] and Peter Luger[†]

[†]*Freie Universität Berlin, Institut für Chemie und Biochemie/Anorganische Chemie, Fabeckstr. 36a, 14195 Berlin, Germany,* [‡]*Julius-Maximilians-Universität Würzburg, Institut für Pharmazie und Lebensmittelchemie, Am Hubland, 97074 Würzburg, Germany, and* [§]*Universität Hamburg, Mineralogisch-Petrographisches Institut, Grindelallee 48, 20146 Hamburg, Germany*

vongrabo@chemie.fu-berlin.de

Received November 1, 2010

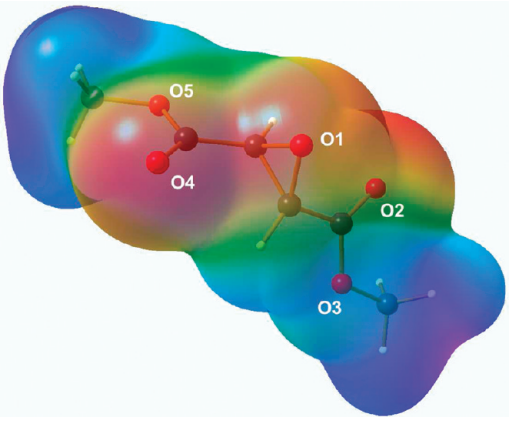

A series of acceptor-substituted epoxide derivatives is scrutinized by means of experimental and theoretical electron-density investigations. Due to the possibility of nucleophilic ring-opening, the epoxide ring is not only a very useful functional group in organic synthesis, but acceptor-substituted epoxides are valuable building blocks for the design of protease inhibitors. Therefore, the electron-density analysis in this work focuses on two main aspects that can contribute to rational drug design: (i) the quantification of the electron-withdrawing substituent effects on the epoxide ring and (ii) the intermolecular interactions involving the epoxide ring in combination with different substituents. It can be shown that the electron-withdrawing properties of the substituents cause an elongation of the C−C bonds in the epoxide rings and the loss of electron density can be measured by an analysis of critical points, atomic charges, and the source function. The different strengths of the substituents are reflected in these properties. Covalent and electrostatic contributions to the intermolecular interactions and thus the lattice energies are depicted on different molecular surfaces.

Introduction

Epoxides (oxiranes, ethylene oxides, oxacyclopropanes) belong to the most widely used functional groups in organic synthesis. The reason is that the high ring strain leads to a synthetically very useful balance between stability and reactivity.[1] For example, epoxides can be opened by nucleophiles in a syn- or antistereoselective manner, and both reactions can take place at the α- or β-position depending on the conditions used. Reductive cleavage or reductive alkylation of epoxides also provide useful synthetic intermediates. Additionally, properly substituted epoxides, e.g., tetracyano epoxide (compound **4** of this study), are starting materials in electrocyclic ring-opening reactions (e.g., 1,3-dipolar

(1) (a) Yudin, A. K. *Aziridines and Epoxides in Organic Synthesis*; Wiley-VCH: Weinheim, 2006. (b) Padwa, A.; Murphree, S. S. *ARKIVOC* **2006**, *3*, 6.

(2) Huisgen, R. *Angew. Chem., Int. Ed.* **1977**, *16*, 572.

DOI: 10.1021/jo102125n Published on Web 01/20/2011

cycloaddition reactions).[2] The application of epoxides is so broad and straightforward that they are a key element of the so-called click-chemistry.[3] There is also a pharmaceutical relevance of epoxides as potential protease inhibitors[4] against various diseases like cancer, stroke, and parasitic or viral diseases. These applications are based on the ring-opening reaction of epoxide derivatives with nucleophilic amino acids (e.g., cysteine,[4] aspartate[5]) of enzymes involved in these diseases, namely proteases responsible for tumor progression and metastasis (e.g., cathepsins B, D, and L),[6] ischemic cell death (calpains),[7] or enzymes essential for the life cycle of the parasites[8] or viruses.[9] We use acceptor-substituted epoxides as model compounds for biologically active agents in this field as the mode of action regarding the recognition and inhibition process with the target enzymes is not sufficiently understood. There are several factors that explain the enzymatic activity of the epoxide agents. Besides the electronic nature of the epoxide ring as the biologically active center of the molecules, the steric interactions of the entire enzyme-ligand aggregation alter the activity by lowering or raising the transition state of the reaction including solvent interactions in the aqueous biological environment. Electron-density investigations can contribute to an explanation of the activity because they provide electronic properties which are important in the molecular association process, e.g., properties describing electrostatic complementarity.[10] High-resolution X-ray diffraction experiments at ultralow temperatures on single crystals resulting in the experimental electron-density distribution are most helpful because the effects of molecular associations are present in a crystalline environment as well as in a protein environment under physiological conditions and can be expected to be comparable in size.[11] On the other hand, electron-density investigations yield deep insight about atomic and bond properties by means of a topological analysis according to Bader (Quantum Theory of Atoms in Molecules[12]). With this method, the degree of covalency/ionicity of a bond can be measured, local charge concentrations and depletions can be found, atomic volumes and charges can be calculated, and electronic communication throughout the molecule can be quantified. This knowledge contributes to a further understanding of reactivity and reaction mechanisms in epoxide chemistry.

The geometrical arrangement of the bonds in the epoxide ring owing to mechanical forces within a ball-and-stick model suggests that the bonds must bend outward to master the high strain (so-called banana bonds[13]). Similar considerations apply for molecular-orbital (MO) and valence-bond (VB) theories, respectively: A nonbent bond scenario is not possible because overlap of ordinary atomic hybrid orbitals can only produce 90° (pure p character) and not 60° as would be necessary for a nonbent bond description. Therefore, ordinary hybridization states, e.g., sp^3 or sp^2, are modified with increased or decreased s-orbital character in order to accommodate a particular molecular geometry. Corresponding models were developed for cyclopropane, but can also be considered for epoxide.[14−16] The Förster−Coulson−Moffitt model[17] makes use of hybrid orbitals with a relation between s- and p-character similar to sp^2-hybridization. This leads to an orbital overlapping outside the direct bond axis forming three σ-type bonds. An alternative model is the Walsh model,[18] in which a stable central three-center bond is formed from inward-directed sp^2 atomic orbitals. Additionally, two weak peripheral three-center bonds are formed from the tangential in-plane p−π orbitals of the CH_2 fragments. The Walsh model does not correspond to the ground state of cyclopropane/epoxide, so that the bent-bond description of the Förster−Coulson−Moffitt model is the commonly considered one.[16] But one could also state that the models describe two different aspects of ring strain. However, the involvement of sp^2-type orbitals in the epoxide ring instead of sp^3 like in a normal single bond suggests that the bonds are not saturated and can interact with π-electron systems. Evidence by various methods (UV spectroscopy, heat of combustion, MO calculations) has been found for such conjugation of the epoxide ring with substituents.[14,19]

Therefore, we are interested to investigate these conjugation effects with electron-density means. We synthesized and crystallized a row of acceptor-substituted epoxide derivatives (see Figure 1a) to study substituent effects caused by conjugation. The resonance formulas that express the conjugation effects with the present electron-withdrawing substituents (cyano, methyl ester and nitrophenyl groups) are given in Figure 1b. The substituents can accept a formal negative charge causing the epoxide ring to open and leaving

(3) (a) Kolb, H. C.; Finn, M. G.; Sharpless, K. B. *Angew. Chem., Int. Ed.* **2001**, *40*, 2004. (b) Fokin, V. V.; Wu, P. *Aziridines and Epoxides in Organic Synthesis*; Wiley-VCH: Weinheim, 2006; Chapter Epoxides and Aziridines in Click Chemistry, p 443.

(4) (a) Powers, J. C.; Asgian, J. L.; Ekici, Ö. D.; James, K. E. *Chem. Rev.* **2002**, *102*, 4639. (b) Otto, H.-H.; Schirmeister, T. *Chem. Rev.* **1997**, *97*, 133. (c) Schirmeister, T.; Klockow, A. *Mini Rev. Med. Chem.* **2003**, *3*, 585.

(5) (a) Dunn, B. M. *Chem. Rev.* **2002**, *102*, 4431. (b) Degel, B.; Staib, P.; Rohrer, S.; Scheiber, J.; Martina, E.; Büchold, C.; Baumann, K.; Morschhäuser, J.; Schirmeister, T. *Chem. Med. Chem.* **2008**, *3*, 302.

(6) Nomura, T.; Katunuma, N. *J. Med. Invest* **2005**, *52*, 1.

(7) Wang, K. *Role of proteases in the pathophysiology of neurodegenerative diseases*; Kluwer Academic/Plenum Publishers: Dordrect, 2002, Chapter Therapeutic approaches with protease inhibitors in neurodegenerative and neurological disorders, p 189.

(8) Kerr, I. D.; Lee, J. H.; Pandey, K. C.; Harrison, A.; Sajid, M.; Rosenthal, P. J.; Brinen, L. S. *J. Med. Chem.* **2009**, *52*, 852.

(9) (a) Lee, T.-W.; Cherney, M. M.; Huitema, C.; Liu, J.; James, K. E.; Powers, J. C.; Eltis, L. D.; James, M. N. G. *J. Mol. Biol.* **2005**, *353*, 1137. (b) Martina, E.; Stiefl, N.; Degel, B.; Schulz, F.; Breuning, A.; Schiller, M.; Vicik, R.; Baumann, K.; Ziebuhr, J.; Schirmeister, T. *Bioorg. Med. Chem. Lett.* **2005**, *15*, 5365. (c) Ro, S.; Baek, S.-G.; Lee, B.; Ok, J.-H. *J. Pept. Res.* **1999**, *54*, 242. (d) Schulz, F.; Gelhaus, C.; Degel, B.; Vicik, R.; Heppner, S.; Breuning, A.; Leippe, M.; Gut, J.; Rosenthal, P. J.; Schirmeister, T. *ChemMedChem* **2007**, *2*, 1214.

(10) (a) Náray-Szabo, G.; Ferenczy, G. G. *Chem. Rev.* **1995**, *95*, 829. (b) Spackmann, M. A.; McKinnon, J. J.; Jayatilaka, D. *CrystEngComm* **2008**, *10*, 377.

(11) Mladenovic, M.; Arnone, M.; Fink, R. F.; Engels, B. *J. Phys. Chem. B* **2009**, *113*, 5072.

(12) (a) Bader, R. F. W. Atoms in Molecules: A Quantum Theory. *The International Series of Monographs on Chemistry*, 1st ed., no. 22; Clarendon Press: Oxford, U.K., 1990. (b) Bader, R. F. W.; Popelier, P. L. A.; Keith, T. A. *Angew. Chem., Int. Ed.* **1994**, *33*, 620. (c) Coppens, P. *Angew. Chem., Int. Ed.* **2005**, *44*, 6810. (d) Koritsánszky, T. S.; Coppens, P. *Chem. Rev.* **2001**, *101*, 1583.

(13) Coulson, C. A. *Valence*, 2nd ed.; Oxford University Press: London, 1963.

(14) Parker, R. E.; Isaacs, N. S. *Chem. Rev.* **1959**, *59*, 737.

(15) Pan, D.-K.; Gao, J.-N.; Lin, H.-L.; Huang, M.-B.; Schwarz, W. H. E. *Int. J. Quantum Chem.* **1986**, *29*, 1147.

(16) Wiberg, K. B. *Acc. Chem. Res.* **1996**, *29*, 229.

(17) (a) Förster, T. *Z. Phys. Chem. B* **1939**, *43*, 58. (b) Coulson, C. A.; Moffitt, W. E. *Phil. Mag.* **1949**, *40*, 1. (c) Coulson, C. A.; Goodwin, T. H. *J. Chem. Soc.* **1962**, 2851.

(18) (a) Walsh, A. D. *Nature* **1947**, *159*, 712. (b) Walsh, A. D. *Trans. Faraday Soc.* **1949**, *45*, 179.

(19) (a) Frolov, Y. L.; Shostakovskii, S. M.; Kagan, G. I. *Teor. Eksp. Khim.* **1969**, *5*, 153. (b) Strait, L. A.; Ketcham, R.; Jambotkar, D.; Shah, V. P. *J. Am. Chem. Soc.* **1964**, *86*, 4628.

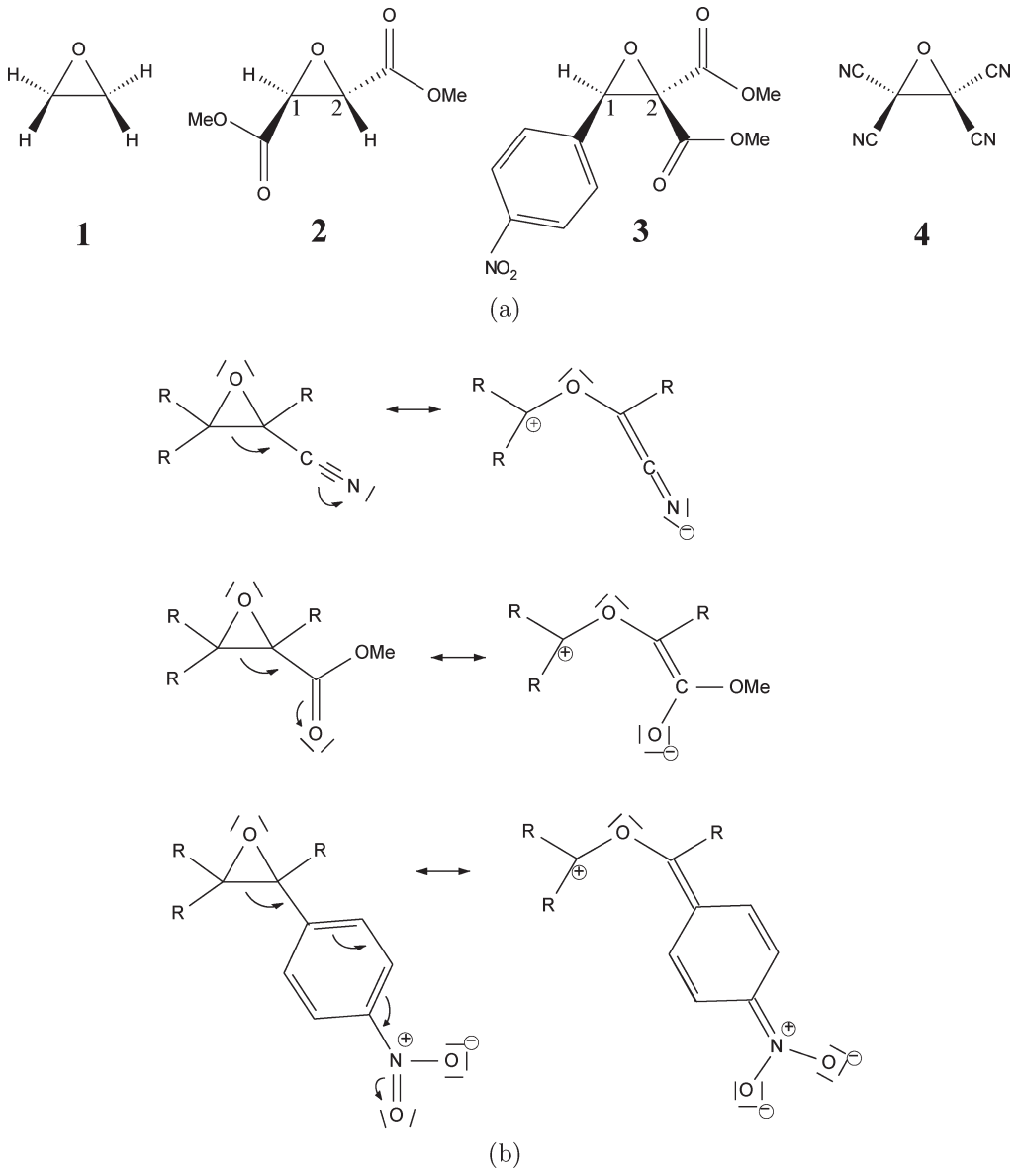

FIGURE 1. (a) Chemical structures of the scrutinized compounds **1** to **4** and (b) selected resonance formulas with the relevant substituents.

a formal positive charge at the farther carbon atom. All groups are commonly considered as being strong acceptors, but the cyano group is definitely the strongest. The first part of the paper will deal with substituent effects on bond-topological and atomic properties; the second part will focus on electrostatics and intermolecular interactions present in the crystal lattices of the acceptor-substituted epoxides. These two aspects are most important for reactivity and biological activity.

Single crystals of compounds **1**−**4** were measured at the in-house diffractometer and at the synchrotron beamline F1 of HASYLAB/DESY in Hamburg, Germany. An aspherical electron-density modeling to account for bonding and non-bonding effects in contrast to the commonly used independent atom approach yielded the total electron-density distribution. Theoretical calculations at the experimental and optimized geometries of the isolated molecules and of the molecules within periodic boundaries were performed to compare theoretical with experimental densities.

The crystal-structure analysis and electron-density determination of unsubstituted epoxide **1** were already published in refs 20 and 21, mainly focusing on technical aspects. Concerning protease inhibition, we first published a study in which we compared different active centers (aziridines, epoxides, and olefins) substituted with identical electron-withdrawing groups (see ref 22). This included the electron-density determination of nitrophenyl-substituted epoxide **3**. In a second step, we investigate the effect of different electron-withdrawing substituents on the same active center (epoxide) in this work. Therefore, two new electron-density studies were carried out (compounds **2** and **4**) and set in a

(20) Luger, P.; Zaki, C.; Buschmann, J.; Rudert, R. *Angew. Chem., Int. Ed.* **1986**, *25*, 276.

(21) Grabowsky, S.; Weber, M.; Buschmann, J.; Luger, P. *Acta Crystallogr. B* **2008**, *64*, 397.

(22) (a) Grabowsky, S.; Pfeuffer, T.; Chęcińska, L.; Weber, M.; Morgenroth, W.; Luger, P.; Schirmeister, T. *Eur. J. Org. Chem.* **2007**, *17*, 2759. (b) Grabowsky, S.; Pfeuffer, T.; Morgenroth, W.; Paulmann, C.; Schirmeister, T.; Luger, P. *Org. Biomol. Chem.* **2008**, *6*, 2295.

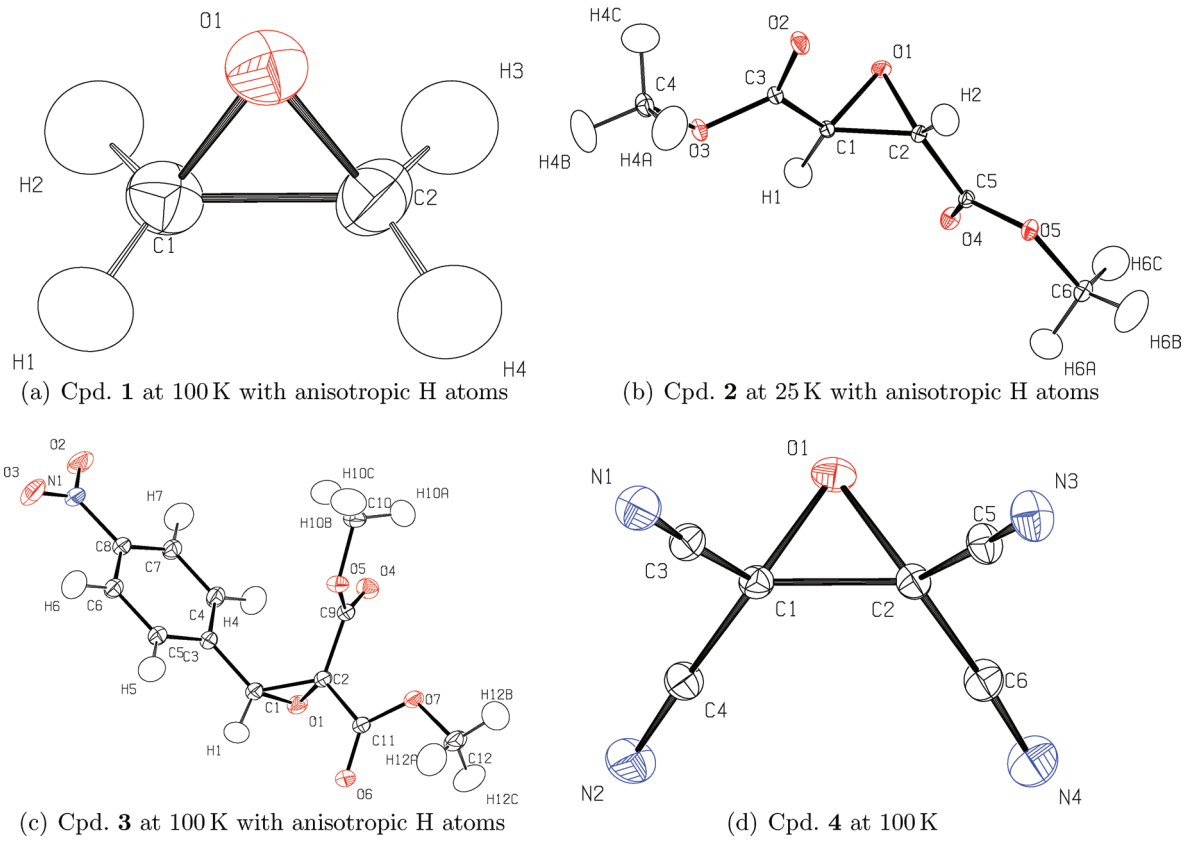

(a) Cpd. **1** at 100 K with anisotropic H atoms

(b) Cpd. **2** at 25 K with anisotropic H atoms

(c) Cpd. **3** at 100 K with anisotropic H atoms

(d) Cpd. **4** at 100 K

FIGURE 2. ORTEP[25] representations of compounds **1**−**4**. Thermal ellipsoids at 50% probability; atomic numbering scheme given. The numbering of the second molecule in the asymmetric unit of compound **2** corresponds to the first one, but the capital letter A is added to each label to relate the atom to the second molecule.

systematic row with the electron densities of compounds **1** and **3**. For the present study, the latter two data sets were re-evaluated, so that all data sets were treated identically using newest available methods like anisotropic displacement parameters for hydrogen atoms or optimized expansion/contraction parameters. A first experimental electron-density study of cyano-substituted epoxide **4** has in fact been published by Matthews et al. already in 1971,[23] but the results are only on a qualitative level. The crystal structure and the electron-density distribution of methyl ester substituted epoxide **2** are not known so far, although this compound is the one directly used as a building block in the rational design of protease inhibitors. In a preceding communication,[24] we introduced the experimental electron localizability indicator (ELI) and applied it to the given series of epoxides as a first case study. Substituent and crystal effects were detected in the new experimental ELI and electron pairs forming the C−O and C−C bonds were found to be localized outside the epoxide ring. In the present paper, these effects are analyzed with various tools of the electron-density research, so that they can be connected to biological activity and reactivity.

(23) (a) Matthews, D. A.; Swanson, J.; Mueller, M. H.; Stucky, G. D. *J. Am. Chem. Soc.* **1971**, *93*, 5945. (b) Matthews, D. A.; Stucky, G. D. *J. Am. Chem. Soc.* **1971**, *93*, 5954.

(24) Grabowsky, S.; Jayatilaka, D.; Mebs, S.; Luger, P. *Chem.—Eur. J.* **2010**, *16*, 12818.

Results and Discussion

1. Substituent Effects. The final structures after multipole modeling are shown in Figure 2, including the atomic numbering scheme. The use of anisotropic displacement parameters for hydrogen atoms can be seen in the ORTEP representations, which improved the density model significantly. There are two molecules in the asymmetric unit of compound **2**. Since their ED properties are very similar, averaged values are used in the discussion unless otherwise stated.

If the open forms of the resonance formulas in Figure 1b have some impact on the situation of the epoxide ring, the C−C bonds should lengthen and the C−O−C angles should widen upon substitution with electron-withdrawing groups (EWGs) compared to unsubstituted compound **1**. The more EWGs are present, the more significant the effect should be. This can be seen unambiguously in Table 1, which summarizes bond lengths and angles for compounds **1**−**4** (complete lists can be found in the Supporting Information). In all three methods (experiment, geometry optimizations within periodic boundary and of the isolated molecule), the bond C1−C2 is shortest for compound **1** (1.46−1.47 Å) and lengthens toward compound **4** (1.50−1.52 Å). Accordingly, the angle C1−O1−C2 widens significantly from compound **1** (60.7−60.9°) to compound **4** (63.5−64.4°). The impact on the C−O bonds and the O−C−C angles is less pronounced, but still present. These findings are in accordance with the high reactivity especially of compound **4** in ring-opening reactions involving C−C bond breaking.

TABLE 1. Selected Bond Distances (Å) and Angles (deg) in Compounds 1−4[a]

bond, angle	1	2	3	4
epoxide ring				
C1−O1	1.434(1)	1.424(2)	1.435(1)	1.426(1)
	1.449	1.431	1.436	1.433
	1.428	1.416	1.426	1.423
C2−O1	1.441(1)	1.427(2)	1.420(1)	1.422(1)
	1.454	1.434	1.428	1.429
	1.428	1.416	1.420	1.424
C1−C2	1.457(1)	1.472(2)	1.488(1)	1.499(1)
	1.468	1.477	1.497	1.519
	1.464	1.479	1.486	1.517
C1−O1−C2	60.91(4)	62.15(8)	62.80(3)	63.54(3)
	60.78	62.06	63.05	64.13
	61.68	62.99	62.95	64.38
O1−C1−C2	59.79(3)	59.03(8)	58.10(3)	58.10(3)
	59.78	59.05	58.22	57.79
	59.15	58.50	58.34	57.81
O1−C2−C1	59.30(3)	58.82(7)	59.09(3)	58.36(3)
	59.44	58.88	58.73	58.08
	59.18	58.51	58.71	57.81
bonds to substituents	C1−H1	C1−H1	C1−H1	C1−C3
	1.099	1.099	1.099	1.450(1)
	1.088	1.085	1.089	1.454
	1.085	1.083	1.085	1.448
	C1−H2	C1−C3	C1−C3	C1−C4
	1.099	1.507(2)	1.487(1)	1.449(1)
	1.089	1.505	1.491	1.453
	1.085	1.504	1.487	1.448
	C2−H3	C2−H2	C2−C9	C2−C5
	1.098	1.099	1.514(1)	1.451(1)
	1.087	1.086	1.518	1.455
	1.085	1.083	1.513	1.448
	C2−H4	C2−C5	C2−C11	C2−C6
	1.099	1.507(2)	1.516(1)	1.450(1)
	1.088	1.506	1.521	1.454
	1.085	1.504	1.521	1.448

[a]First row, experiment; second row, periodic-boundary optimization; third row, isolated-molecule optimization; C−H bonds fixed to averaged neutron-diffraction values in the experimental case.

In the second part of Table 1, the bonds of the ring carbon atoms to the four substituents of the epoxide ring are listed. C−H distances range from 1.085 to 1.089 Å for the two geometry optimizations and were fixed to 1.099 Å from averaged neutron-diffraction values within the experimental geometries. The C−C bonds can clearly be distinguished with respect to the different EWGs. In the resonance formulas in Figure 1b, the C−C bonds are assigned partial double-bond character and should therefore shorten according to the electron-withdrawing capability of the corresponding EWG. Consequently, the C−C bonds in compound **4** are shortest since the cyano groups are the strongest EWGs. The bond C1−C3 to the nitro-phenyl group in compound **3** is second shortest, indicating that this group is the second strongest EWG. The bonds to the methyl ester groups in compounds **2** and **3** are longest. In summary, the geometrical effects expected from the resonance formulas can clearly be found and confirm that the substituent effects are significant and detectable.

Experimental deformation density and Laplacian maps in the plane of the epoxide ring are shown in Figure 3. The maxima of the deformation density and the valence shell charge concentrations (VSCCs) in the Laplacian maps are located clearly outside the bond axes for both the C−O and C−C bonds, and there are no maxima inside the ring. This favors the description of bent bonds according to the Förster−Coulson−Moffitt model, which was already experimentally found for cyclopropane before.[26] However, the C−O bond critical points (bcps) from a topological analysis of the ED according to Bader[12] are located directly on the bond axes, but the bond paths are curved in an S-type shape. For details on this point and a comparison with the electron localizability indicator, see ref 24.

Here, the effects of the EWGs on the density distribution will be discussed. Therefore, the most differing experimental maps are shown, which agree well with theoretically calculated maps. The maps of the three symmetrically substituted compounds **1**, **2**, and **4** are generally identical. The distribution of deformation density and Laplacian mirrors the symmetrical substitution pattern as given in parts a and c of Figure 3 for compound **2**. For unsymmetrically substituted compound **3** (parts b and d of Figure 3), the maps mirror the asymmetry. The bond C2−O1 seems to be weaker and more ionic than C1−O1; C2 carries two EWGs, whereas C1 carries only one EWG.

The approach of Bader to topologically analyze the ED yields, among others, bond-topological and atomic properties.[12] Bond-topological properties are the values of the ED and the Laplacian at the bond critical points (bcps); atomic charges and volumes result from an integration of the ED over the volume enclosed by the zero-flux surfaces. Electron density and Laplacian values at the bcps of C−O and C−C bonds in the epoxide rings are plotted in Figure 4a. Comparisons between the four different compounds, but also between the five different methods employed, can be made from these plots. Complete lists of values for all bonds are given in the Supporting Information. The most important chemical effect concerns the bond C1−C2. According to the lengthening of this bond from compound **1** to compound **4**, the values of the ED at the C1−C2 bcps as well as the negative Laplacian decrease, Figure 4a, right block. The effect is most clearly visible in the isolated-molecule calculations at experimental geometry. The ED decreases from 1.81 e Å^{-3} (compound **1**) over 1.73 e Å^{-3} (compound **2**) and 1.68 e Å^{-3} (compound **3**) to 1.65 e Å^{-3} (compound **4**). Corresponding values for the Laplacian are −16.7, −14.6, −13.2, and −12.4 e Å^{-5}. This can be interpreted as a loss of covalency of the C−C bond as it loses electron density to the substituents. This is the explanation why compound **4** is a very good substrate for the above-mentioned electrocyclic ring-opening reactions.

Besides this expected chemical effect for C1−C2, the most striking feature in Figure 4a is that the differences between the methods are larger than the differences between the compounds. Whereas the agreement between the methods is in a typical range for the ED (smaller than 0.1 e Å^{-3}),[27] the differences are large in the Laplacian. The negative Laplacian values from multipole-free isolated-molecule calculations are

(25) Burnett, M. N.; Johnson, C. K. *ORTEP-III*, *Oak Ridge* Thermal Ellipsoid Plot Program for Crystal Structure Illustrations, Oak Ridge National Laboratory Report ORNL-6895, Oak Ridge, TN, 1996.

(26) (a) Chakrabarti, P.; Seiler, P.; Dunitz, J. D.; Schlüter, A.-D.; Szeimies, G. *J. Am. Chem. Soc.* **1981**, *103*, 7378. (b) Boese, R.; Miebach, T.; de Meijere, A. *J. Am. Chem. Soc.* **1991**, *113*, 1743. (c) Koritsánszky, T.; Buschmann, J.; Luger, P. *J. Phys. Chem.* **1996**, *100*, 10547. (d) Luger, P.; Messerschmidt, M.; Scheins, S.; Wagner, A. *Acta Crystallogr. A* **2004**, *60*, 390.

(27) Grabowsky, S.; Kalinowski, R.; Weber, M.; Förster, D.; Paulmann, C.; Luger, P. *Acta Crystallogr. B* **2009**, *65*, 488.

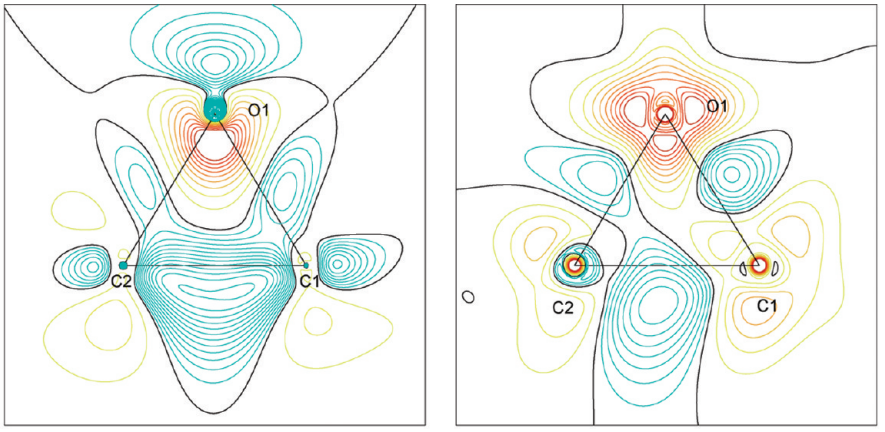

(a) Deformation density of cpd. **2**, contour interval = 0.025 e Å^{-3} (b) Deformation density of cpd. **3**, contour interval = 0.04 e Å^{-3}

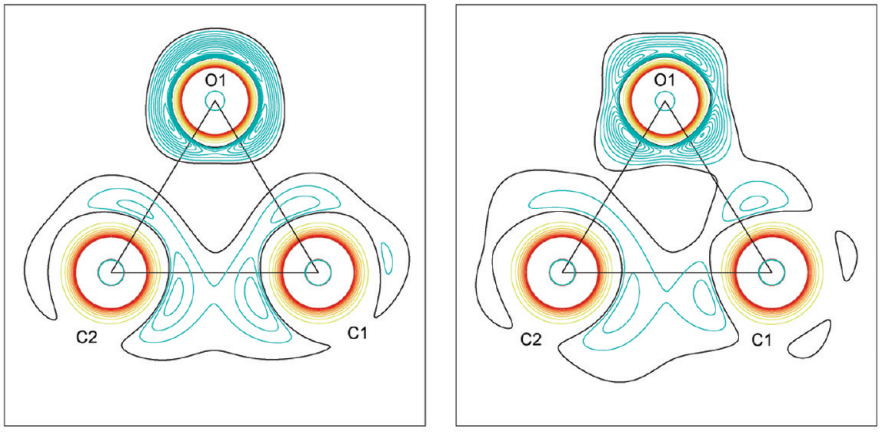

(c) Laplacian of cpd. **2**, contour interval = 7 e Å^{-5} (d) Laplacian of cpd. **3**, contour interval = 9 e Å^{-5}

FIGURE 3. Experimental static deformation−density and Laplacian−distribution maps in planes of the epoxide ring. Deformation−density maps: blue = positive, red = negative, black = zero; Laplacian-distribution maps: blue = negative, red = positive, black = zero.

significantly larger than the ones from multipole modeling of experimental or theoretical (periodic boundary) structure factors. This is due to inconsistencies of the multipole model especially for strained and polar bonds.[28]

The strained situation of the epoxide ring cannot be detected in the values of the ED and the Laplacian at the C−O and C−C bcps. The range of values covered by these bonds is the same as can be found for C−O bonds in nonstrained C−O−C linkages or nonstrained C−C bonds (compare, for example, ref 29). However, the bond strain is reflected in the values of the ellipticity at the bcps. For nonstrained C−O and C−C single bonds, the values are close to zero. For C−O and C−C bonds in epoxide, the values are significantly larger, indicating bent single bonds. They vary between 0.21 and 0.73, see the Supporting Information for details.

Atomic properties of the atoms in the epoxide ring are shown in Figure 4b. Oxygen atoms in the epoxide rings are negatively charged by −0.53 to −0.89 e, and their volumes V_{001} range from 14.1 to 16.7 Å^3. For carbon atoms, corresponding values are Q = 0.15 to 0.61 e and V_{001} = 6.0 to 10.7 Å^3. Carbon atoms C1 and C2 in cyano-substituted epoxide compound **4** are significantly more positive than in the other compounds because they are bonded to the strongest EWGs. The expected trend that is caused by the electron-withdrawing effect of the substituents can best be seen for the volumes of the C2 atoms. The largest volumes (about 10 Å^3 as averaged over all methods) can be found for unsubstituted compound **1**. It decreases to about V_{001} = 8 Å^3 in compound **2**, in which C2 is bonded to one methyl ester group, and again decreases to about V_{001} = 7 Å^3 in compound **3**, where C2 is bonded to two methyl ester groups. Finally, V_{001} is about 6 Å^3 in compound **4**. In contrast to the Laplacian values discussed above, this effect is much larger than the differences between the different methods.

The total charge of the epoxide ring is significantly negative for compound **1** and significantly positive for compound **4** regardless of the method; compounds **2** and **3** range in-between. This again confirms the order of the electron-withdrawing strength of the substituents. The effect is most pronounced for the experiment and least pronounced for the isolated-molecule calculations, compare tables in the Supporting Information. In the experiment, the epoxide ring is

(28) (a) Volkov, A.; Abramov, Y.; Coppens, P.; Gatti, C. *Acta Crystallogr. A* **2000**, *56*, 332. (b) Henn, J.; Ilge, D.; Leusser, D.; Stalke, D.; Engels, B. *J. Phys. Chem. A* **2004**, *108*, 9442.

(29) Jaradat, D. M. M.; Mebs, S.; Checińska, L.; Luger, P. *Carbohydr. Res.* **2007**, *177*, 149.

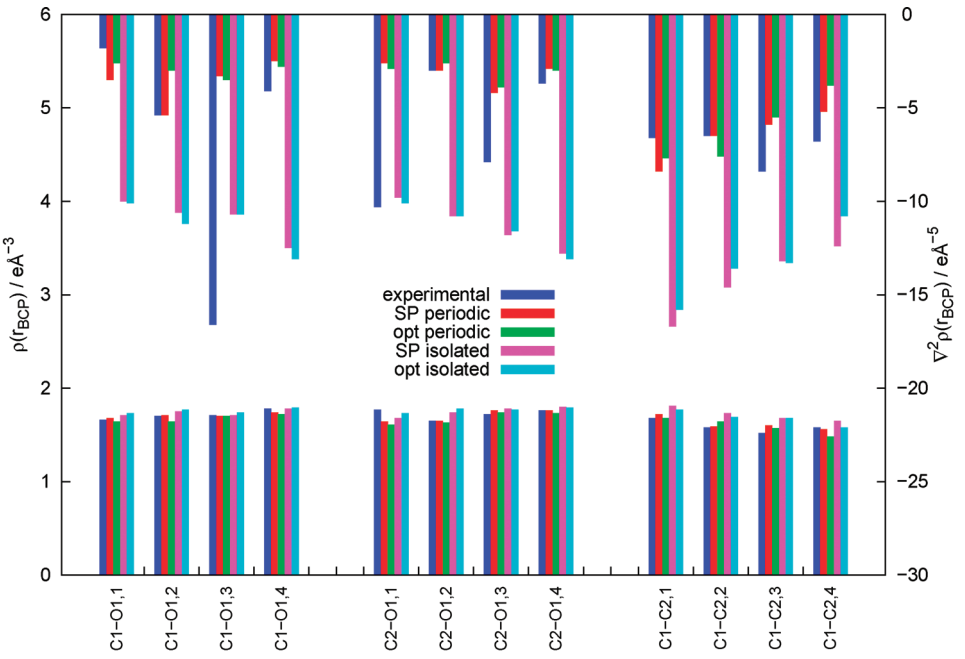

(a) Bars pointing from bottom to top refer to ED values ϱ(bcp) (left y-axis), bars from top to bottom refer to the Laplacian $\nabla^2\varrho$(bcp) (right y-axis)

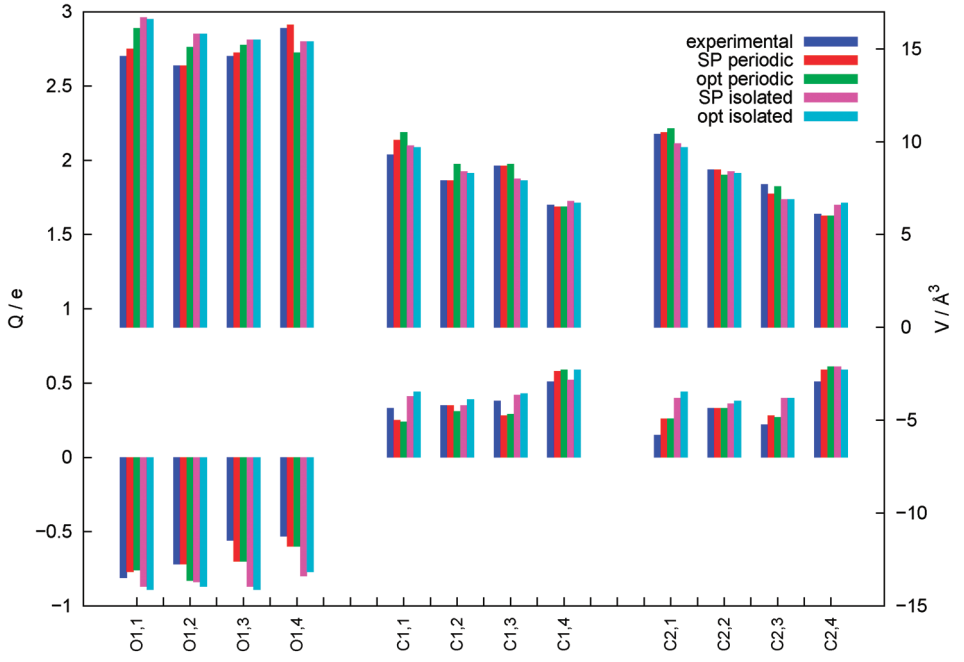

(b) Bars in the lower half refer to charges Q (left y-axis), bars in the upper half refer to volumes V_{001} (right y-axis)

FIGURE 4. Bond−topological and atomic properties within the epoxide rings of compounds **1**−**4**. Labeling 1−4 refers to compounds **1**−**4**; experimental, SP/opt periodic = periodic−boundary calculations at experimental/optimized geometry, SP/opt isolated = isolated−molecule calculations at experimental/optimized geometry.

charged by −0.33 e for compound **1** (unsubstituted), by −0.04 e for compound **2** (two EWGs), by 0.04 e for compound **3** (three EWGs), and by 0.49 e for compound **4** (four EWGs). In summary, the effects of the EWGs can be detected in bond-topological and atomic properties as expected from the order of the electron-withdrawing capabilities of the substituents despite methodological and experimental uncertainties.

The source function is a recently introduced tool within the framework of the topological analysis of ED to quantify electronic communication within a molecule. Bader and Gatti showed that the electron density at any point $\vec{r}$ (called reference point) within a molecule consists of contributions from a source operating at all other points $\vec{r}'$.[30] Therefore, it is possible to calculate the contributions of each

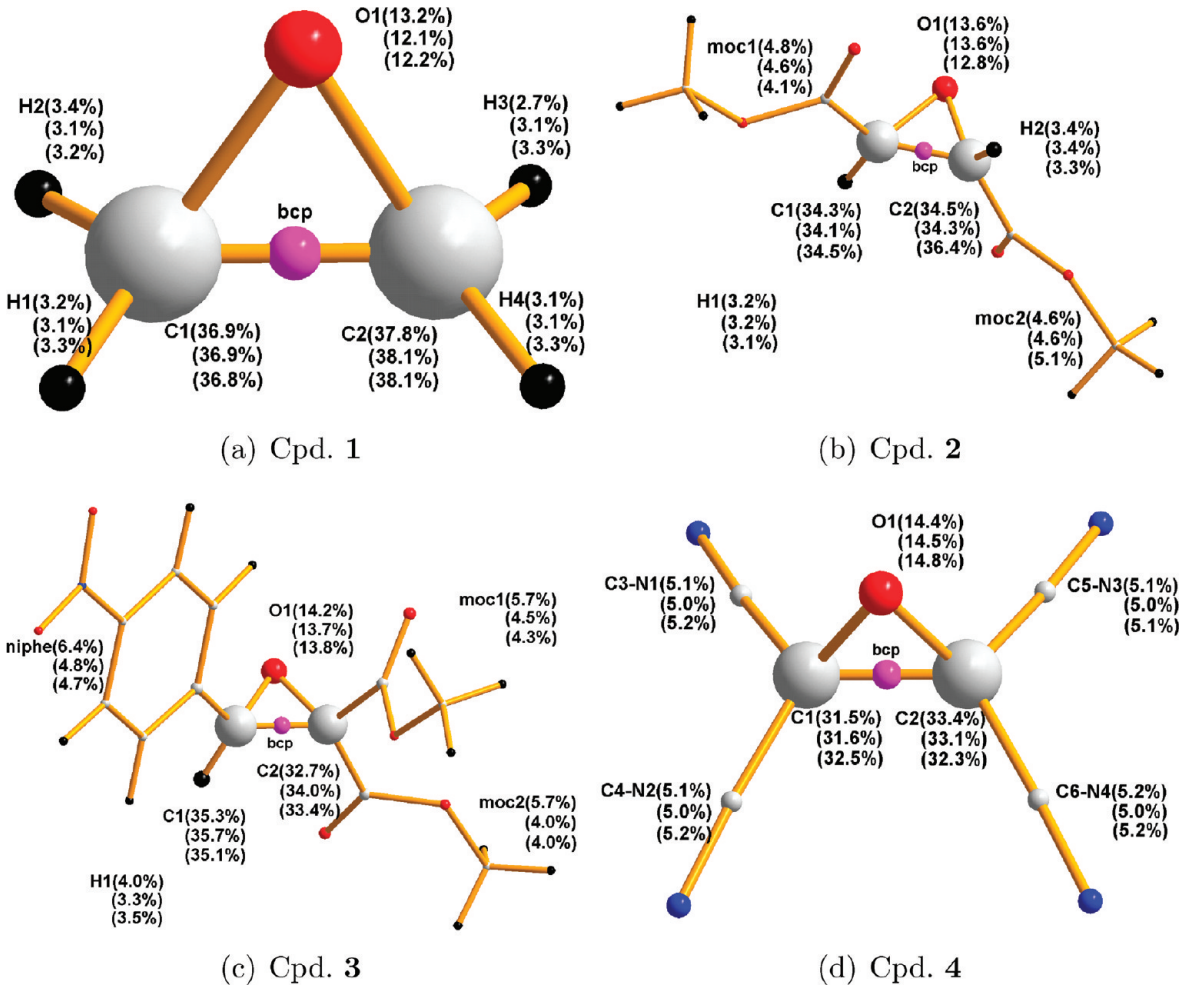

FIGURE 5. Relative atomic contributions to the ED of the C−C bonds in the epoxide rings from the source function of compounds **1**−**4**. First value = experiment; second/third value = periodic-boundary calculations at experimental/optimized geometry, relative source contributions of the atoms to the plotted bcps are represented by the atoms' radii; color code only indicates atom type.

atomic basin to the ED at, for example, a bcp characterizing a bond. In Figure 5, we show a representation of the source contributions of all atoms in the molecules to the C−C bcp in the epoxide ring; the absolute numbers and a corresponding representation for the C−O bonds can be found in the Supporting Information.

Substituent effects can be detected in the source function in the usual order from compound **1** without EWGs to compound **4** with four strongest EWGs: In compound **1**, about 75% of the density at the C1−C2 bcp originates from the directly bonded atoms. This contribution decreases upon substitution with methyl ester and nitrophenyl groups. The sum of C1 and C2 contributions is about 69% in both compounds **2** and **3**. In cyano-substituted epoxide **4**, the value significantly decreases again (about 65%). The contributions of the EWGs are larger (averaged to 4.7% for a methyl ester group, 5.3% for the nitrophenyl group and 5.1% for a cyano group) than the contributions of a hydrogen atom (averaged to 3.3%). In other words, the electron-withdrawing groups donate more ED to the bcp of the C−C bond than the hydrogen atoms. This paradox can only be explained by the fact that resonance effects are not reflected in the source function with the bcp as reference point. This was also found by Farrugia and Macchi recently.[31] They stated that "...when the reference point is close to the nodal plane of an orbital, this orbital makes a low to negligible contribution to the SF (source function), which has clear implications for the interpretation of π-interactions. This leads us to recommend caution in associating some chemical concepts with features of the SF...". As the epoxide ring is unsaturated and contains sp^2-like hybrid orbitals, the resonance formulas in Figure 1b can be explained with π-interactions. Therefore, the resonance effects of the present substituents on the epoxide ring cannot be characterized by means of the source function.

However, substituent effects due to inductive effects can still be found. Considering also the C−O bcps as reference points (see the Supporting Information), the difference between a carbon atom in the epoxide neighboring a C−O bond and an oxygen atom neighboring the C−C bond becomes clear. Oxygen is the better donor in terms of source contributions, its contributions are about twice as high. But

(30) (a) Bader, R. F. W.; Gatti, C. *Chem. Phys. Lett.* **1998**, *287*, 233. (b) Gatti, C.; Cargnoni, F.; Bertini, L. *J. Comput. Chem.* **2003**, *24*, 422. (c) Gatti, C.; Bertini, L. *Acta Crystallogr. A* **2004**, *60*, 438.

(31) Farrugia, L. J.; Macchi, P. *J. Phys. Chem. A* **2009**, *113*, 10058.

carbon is still a better donor than a hydrogen atom, so the donating capabilities seem to be in the order of the electronegativity of the elements. Consequently, the contributions of the directly bonded atoms change according to the electronegativities of the adjacent atoms. This can most clearly be found for the carbon atom C2 in Figure 5 (consider values from periodic-boundary calculations at optimized geometry). C2 contributes 38.1% to the C1−C2 bcp in compound **1** with two adjacent hydrogen atoms. The contribution decreases to 36.4% in compound **2** with one adjacent hydrogen atom and one more electronegative sp^2 carbon atom. It again decreases to 33.4% in compound **3** with two adjacent sp^2 carbon atoms. In cyano-substituted compound **4**, the contribution is only 32.3% because C2 is adjacent to two sp carbon atoms, which are more electronegative than sp^2 carbon atoms.

2. Intermolecular Interactions. There are no classical hydrogen-bond donor groups like O−H or N−H in compounds **1**−**4**. In cyano-substituted epoxide compound **4**, there are not even hydrogen atoms. Therefore, the discussion on intermolecular interactions is about C−H···O hydrogen bonds and N···C contacts. Compound **1** exhibits three C−H···O interactions so that the hydrogen-bonding pattern is unsymmetrical, which is reflected in differing C−O distances and O−C−C angles. In the optimized geometry from a periodic-boundary calculation, the hydrogen bond C1−H1···O1 does not exist, but C2−H3···O1 exists instead, which is in turn not present in the experimental lattice, see Table 2. In compounds **2** and **3**, numerous C−H···O hydrogen bonds are present, but only ester and nitro oxygen atoms are acceptors and not the epoxide oxygen atom O1. In compound **4**, there are many N···C contacts with several bcps and rcps, but only the two ones that are shorter than 3.0 Å will be discussed in the following for comparison with the C−H···O hydrogen bonds.

Table 2 lists properties of intermolecular contacts of compounds **1**−**4**. In compounds **2** and **4**, the pattern is identical between experiment and geometry optimization, only strength and direction vary. For compound **3**, there is an additional hydrogen bond (C10−H10A···O4) in the optimized crystal lattice. But for compound **1**, the lattice changes almost completely upon optimization. As already mentioned, C1−H1···O1 only exists in the experiment and C2−H3···O1 only in the optimized case. Moreover, the contact C2−H4···O1 originates from another symmetry operation.

In general, the strength of the C−H···O hydrogen bonds by means of interaction energies (E_{int}) and electron density at the bcp (ρ_{bcp}) is typical for these kinds of interactions. E_{int} are close to −10 kJ mol^{-1} or lower (absolute values), ρ(bcp) varies between 0.03 and 0.09 e Å^{-3}. But the C−H···O interactions in compound **1** with the epoxide oxygen atom as acceptor are slightly weaker, indicated by both E_{int} and ρ_{bcp}, than in compounds **2** and **3** with ester and nitro oxygen atoms as acceptors. The N···C contacts in compound **4** are exactly within the ranges given above, while the distances of these contacts are larger than H···O distances due to a larger sum of the van der Waals radii.

Optimization of the crystal structures does not necessarily lead to closer and stronger intermolecular contacts. Changes of up to 0.2 Å in H···O or C···O distances, 10° in C−H···O angles, 4 kJ mol^{-1} in interaction energies, and not more than 0.03 e Å^{-3} in ρ(bcp) and 0.3 e Å^{-5} in $\nabla^2\rho$(bcp) occur, but in both directions. The values of the ED and the Laplacian at the H···O bcps are closer between experiment and periodic-boundary calculations at experimental geometry than between the two theoretical methods, but this is not true for the interaction energies, which spread more widely.

In biologically interacting systems, mutual recognition of the involved species plays an outstanding role. Since the first step of the recognition process takes place via the molecular surfaces, we have calculated different types of molecular surfaces: isosurfaces of the electron density,[32] Hirshfeld surfaces,[33] and isosurfaces of the electrostatic potential (ESP). The electrostatic potential mapped on ED isosurfaces depicts electrostatic contributions to intermolecular interactions, whereas the ED mapped on Hirshfeld surfaces gives an impression of covalent contributions to the same interactions. ESP isosurfaces in turn help to identify active regions of the molecules.

In the ESP representation of compound **1** on an ED isosurface of 0.0067 e Å^{-3} = 0.001 au (Figure 6a), which corresponds to the molecular van der Waals envelope,[32] the contacts of H1 and H4 are clearly visible as pronounced positive regions (about 0.38 e Å^{-1}). Around oxygen atom O1, there is a continuous distribution of negative ESP with a magnitude of about −0.10 e Å^{-1}. On the Hirshfeld surface (Figure 6b), individual and directed contacts are also visible at the oxygen atom. H1, H2 and H4 exhibit contacts with covalent contributions up to 0.07 e Å^{-3} on the Hirshfeld surface (more than at the bcps, which are minima in the ED along the direction of the interaction), whereas H3 only shows a weak coloring, which exemplifies that there is no C2−H3···O1 interaction of reasonable strength in the experiment.

The experimental ESP of compound **4** was mapped on an ED isosurface of 0.5 e Å^{-3} (Figure 6c), which is much closer to the nuclei. Therefore, the scale of the ESP is shifted toward much more positive values. However, it is obvious that the nitrogen atoms are more negatively polarized than the oxygen atom. Around carbon atoms in the cyano groups and in the epoxide ring, regions of strong positive polarization are located. Thus, N···C contacts guide the crystal packing of this compound. In the corresponding Hirshfeld representation (Figure 6d), these contacts are visualized. Each nitrogen atom is involved in contacts (only a selection is given in Table 2). Instead of a localized charge accumulation, which is always found for classical hydrogen bonds, the Hirshfeld surface close to the carbon atoms is covered by large areas of ED being donated from the nitrogen atoms. The strengths of these interactions are comparable to the C−H···O interactions in the other compounds, compare Table 2 and the scales in Figures 6b and 7b,d.

The analysis of intermolecular interactions is even more important for compound **2** because it is a well-known building block for protease inhibitors; see the Introduction. It is thus an important finding that the experimental ESP of compound **2** in Figure 7a is not distributed in a simple manner (which would be positive at each hydrogen atom, negative at each oxygen atom). There is a belt region of

(32) (a) Bader, R. F. W.; Carroll, M. T.; Cheeseman, J. R.; Chang, C. *J. Am. Chem. Soc.* **1987**, *109*, 7968. (b) Politzer, P.; Murray, J. S.; Preralta-Inga, Z. *Int. J. Quantum Chem.* **2001**, *85*, 676.

(33) (a) Spackman, M. A.; Byrom, P. G. *Chem. Phys. Lett.* **1997**, *267*, 215. (b) McKinnon, J. J.; Mitchell, A. S.; Spackman, M. A. *Chem.—Eur. J.* **1998**, *4*, 2136.

TABLE 2. Selected Properties of Intermolecular Interactions of Compounds 1−4[a]

labels	H···A	D···A	D-H···A	ϱ_{bcp}	$\nabla^2\varrho_{bcp}$	E_{int}	sym
compd **1**:							
C1−H1···O1	2.584	3.579	150.20	0.03(1)	0.5(1)	−3.56	$^1/_2 + x$, $^3/_2 - y$, $^1/_2 + z$
SP periodic				0.05	0.6	−1.45	
opt periodic							
C1−H2···O1	2.520	3.481	145.42	0.05(1)	0.7(1)	−4.29	$^1/_2 - x$, $^1/_2 + y$, $^1/_2 - z$
SP periodic				0.06	0.7	−5.56	
opt periodic	2.453	3.470	154.89	0.07	0.7	−5.58	
C2−H3···O1							
SP periodic							
opt periodic	2.502	3.377	136.73	0.06	0.8	−4.90	$-x$, $-y$, $-z$
C2−H4···O1	2.519	3.503	148.39	0.03(1)	0.5(1)	−4.78	$-^1/_2 + x$, $^3/_2 - y$, $^1/_2 + z$
SP periodic				0.05	0.6	−4.52	
opt periodic	2.596	3.529	143.40	0.05	0.5	−4.43	$-^1/_2 + x$, $-^1/_2 - y$, $^1/_2 + z$
compd **2**:							
C2−H2···O5	2.352	3.391	157.28	0.07	1.0	−4.72	$1 - x$, y, $1 - z$
SP periodic				0.07	1.0	−4.85	
opt periodic	2.351	3.410	164.32	0.08	0.9	−4.78	
C4−H4B···O4	2.543	3.602	172.38	0.06	0.6	−9.89	$^1/_2 - x$, $^1/_2 + y$, $1 - z$
SP periodic				0.06	0.6	−10.25	
opt periodic	2.380	3.465	175.01	0.08	0.9	−6.84	
C6−H6A···O4	2.689	3.647	149.55	0.05	0.5	−11.51	x, $1 + y$, z
SP periodic				0.05	0.5	−12.64	
opt periodic	2.644	3.580	143.55	0.05	0.6	−10.04	
...							
compd **3**:							
C5−H5···O2	2.446	3.486	160.35	0.07	0.6	−5.62	x, $-1 + y$, z
SP periodic				0.06	0.7	−8.58	
opt periodic	2.554	3.607	162.98	0.05	0.5	−5.50	
C6−H6···O5	2.282	3.248	147.30	0.09	0.8	−11.70	$1 - x$, $1 - y$, $1 - z$
SP periodic				0.09	1.0	−10.40	
opt periodic	2.422	3.367	145.08	0.06	0.8	−8.14	
C7−H7···O6	2.264	3.150	137.65	0.09	1.2	−7.22	x, $1 + y$, z
SP periodic				0.08	1.1	−11.44	
opt periodic	2.318	3.197	137.23	0.08	1.0	−8.80	
C10−H10A···O4							
SP periodic							
opt periodic	2.571	3.534	147.06	0.05	0.6	−6.49	$2 - x$, $1 - x$, $-z$
...							
compd **4**:							
N1···C5	2.932			0.08	0.9	−7.77	x, $^3/_2 - y$, $^1/_2 + z$
SP periodic				0.07	0.9	−9.88	
opt periodic	3.107			0.06	0.8	−11.00	
N2···C4	2.993			0.07	0.8	−8.72	$-x$, $-^1/_2 + y$, $^1/_2 - z$
SP periodic				0.06	0.8	−11.27	
opt periodic	3.272			0.05	0.8	−9.34	

[a]Hydrogen···acceptor (H···A) or N···C distance in Å, donor···acceptor (D···A) distance in Å, donor−hydrogen···acceptor (D−H···A) angle in deg, electron density ρ at H···A or N···C bcp in e Å^{-3}, Laplacian $\nabla^2\rho$ at H···A or N···C bcp in e Å^{-5}, interaction energies E_{int} in kJ mol^{-1}, symmetry operation to generate second molecule; for compounds **2** and **3**, only a selection is given here; a complete list can be found in the Supporting Information.

distinctive negative potential spanning obliquely over the epoxide ring connecting the two ester groups (compare also the Table of Contents graphic showing the ESP of compound **2** mapped on the van der Waals ED envelope). This belt region might play a substantial role in the biological mode of action of compound **2**—or, since this belt region can also be found in compound **3** (Figure 7c), generally of compounds incorporating methyl ester groups bonded to an epoxide ring—because the belt regions represent the main nucleophilic sites of the molecules. Oxygen atoms which do not lie in these belt regions are polarized much more positively and are therefore far less nucleophilic. It can best be seen for oxygen atom O3 in compound **2** (Figure 7a), but also holds for atom O5 in compound **3** (Figure 7c). In contrast, the oxygen atoms O1 in the epoxide rings are involved in the negative belt region, but they are no acceptors for hydrogen bonds.

The Hirshfeld representation of compound **2** (Figure 7b) additionally shows an accumulation of interactions in a region corresponding to the belt region in the ESP with oxygen atoms O1, O2, O4, and O5 involved. Oxygen atom O3, which is polarized less negatively and therefore not included in the belt region, actually forms only one weak contact in contrast to the other oxygen atoms. This confirms that intermolecular interactions mainly take place in the belt region, which can therefore be referred to as the active region concerning noncovalent intermolecular interactions. Epoxide oxygen atom O1 is also involved in intermolecular interactions, as displayed on the Hirshfeld surface, as there is a large region of ED above O1. But no hydrogen bond to O1 could be localized by means of a bcp. In compound **3**, the interactions are spread more widely on the Hirshfeld surface (Figure 7d), which is consistent

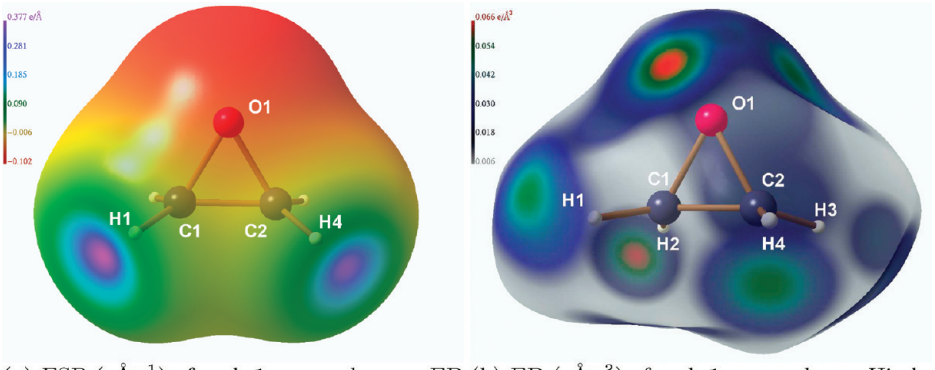

(a) ESP ($eÅ^{-1}$) of cpd. **1** mapped on an ED isosurface of 0.0067 $eÅ^{-3}$ (b) ED ($eÅ^{-3}$) of cpd. **1** mapped on a Hirshfeld surface

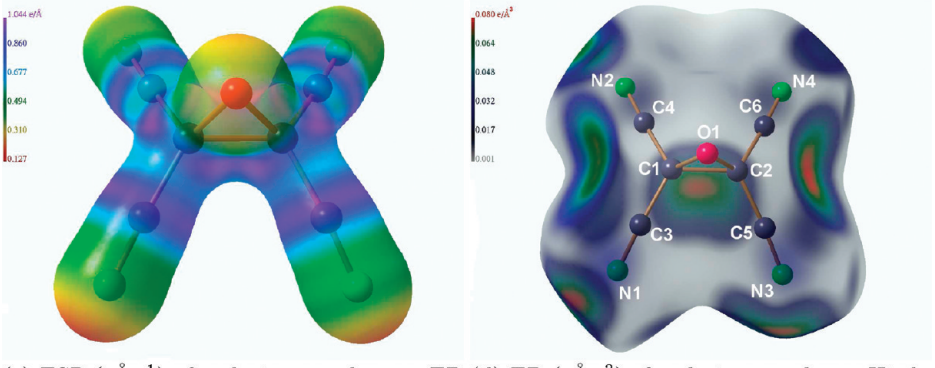

(c) ESP ($eÅ^{-1}$) of cpd. **4** mapped on an ED isosurface of 0.5 $eÅ^{-3}$ (d) ED ($eÅ^{-3}$) of cpd. **4** mapped on a Hirshfeld surface

FIGURE 6. Representations of the experimental electrostatic potentials (ESPs) and the experimental Hirshfeld surfaces of compounds **1** and **4**.

with the fact that compound **2** is biologically active, but compound **3** is much less active regarding nucleophilic ring-opening by a protease. The search for electrophilic and nucleophilic sites within compound **3** compared to aziridine and olefin analoga was the topic of another study; see ref 22.

Lattice energies of compounds **1** to **4** are listed in Table 3. The exchange-repulsion and dispersion terms of the lattice energy are calculated according to the method of Williams and Cox for light atoms.[34] The electrostatic energy is calculated according to the exact potential/multipole moment hybrid method (EPMM) after Volkov.[35] It was discussed above (see, e.g., Table 2) that the number of hydrogen bonds in compound **1** is smallest and they are weakest. Correspondingly, the lattice energy of compound **1** is lowest, too. The lattice energy for one molecule of compound **2** is about twice as high as there are more acceptors for hydrogen bonds, which are stronger than in compound **1**. The hydrogen-bonding networks of the two independent molecules in the asymmetric unit of compound **2** are not identical, which is reflected in the fact that the lattice energy of molecule 1 is significantly higher than that of molecule 2 (up to 25 kJ mol^{-1}). Compound **3** was substituted with a nitrophenyl group not only because of its electron-withdrawing capabilities but also because of the additional introduction of two hydrogen-bond acceptor atoms. The resulting enhanced crystallizing properties are directly reflected in the lattice energy of compound **3**, which is twice as high as for compound **2** and four times as high as for compound **1**. The N···C contacts in compound **4** lead to a lattice energy similar to compound **2**. This means that the absence of hydrogen atoms does not lead to a weaker crystal lattice but that the N···C contacts are considerably strong intermolecular interactions, too. In all compounds, electrostatic contributions dominate the crystal packing, but in compound **3** they are only slightly larger than 50% because absolute values of the exchange−repulsion−dispersion term are much larger for compound **3** than for the other compounds.

Conclusions

In a combined experimental−theoretical approach, the electron-density distributions of four epoxide derivatives with electron-withdrawing substituents were analyzed with respect to the substituent effects and the intermolecular interaction patterns. The order of the influence of the electron-withdrawing groups on the epoxide ring caused by their increasing number and strength could be determined from geometrical, bond-topological and atomic properties. The C−C bond lengthens and the C−O−C angle widens upon substitution with EWGs. Due to a loss of electron density at the bond critical points caused by the electron-withdrawing nature of the substituents, the C−C bonds inside the epoxide ring become less covalent. This is most pronounced in compound **4** and fits to the reactivity of this epoxide in electrocyclic ring-opening reactions. In general,

(34) Williams, D. E.; Cox, S. R. *Acta Crystallogr. B* **1984**, *40*, 404.
(35) Volkov, A.; Koritsánzky, T.; Coppens, P. *Chem. Phys. Lett.* **2004**, *391*, 170.
(36) Mebs, S.; Lüth, A.; Luger, P. *Bioorg. Med. Chem.* **2010**, *18*, 5965.

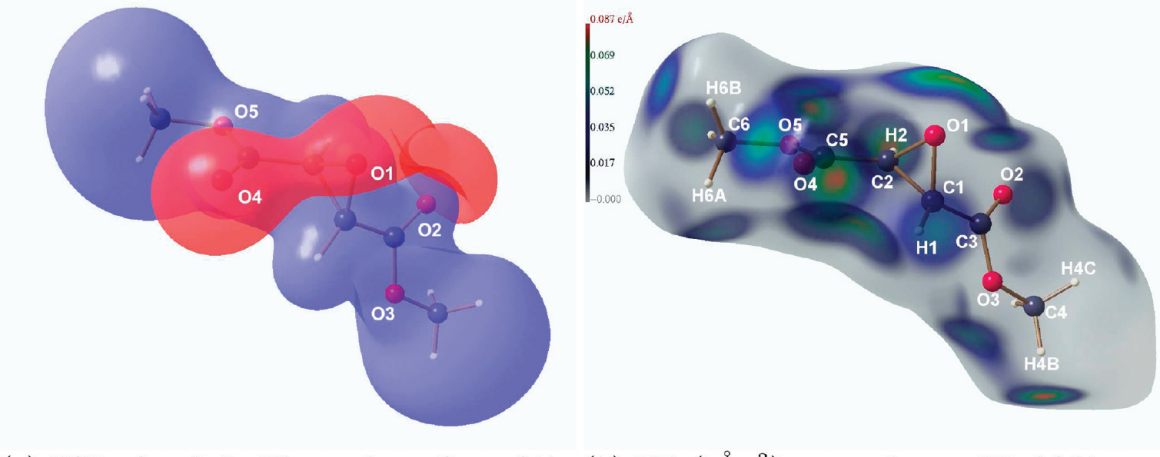

(a) ESP of cpd. **2**: Blue = isosurface of the ESP at 0.1 eÅ^{-1}, red = isosurface of the ESP at -0.1 eÅ^{-1}

(b) ED (eÅ^{-3}) mapped on a Hirshfeld surface of cpd. **2**

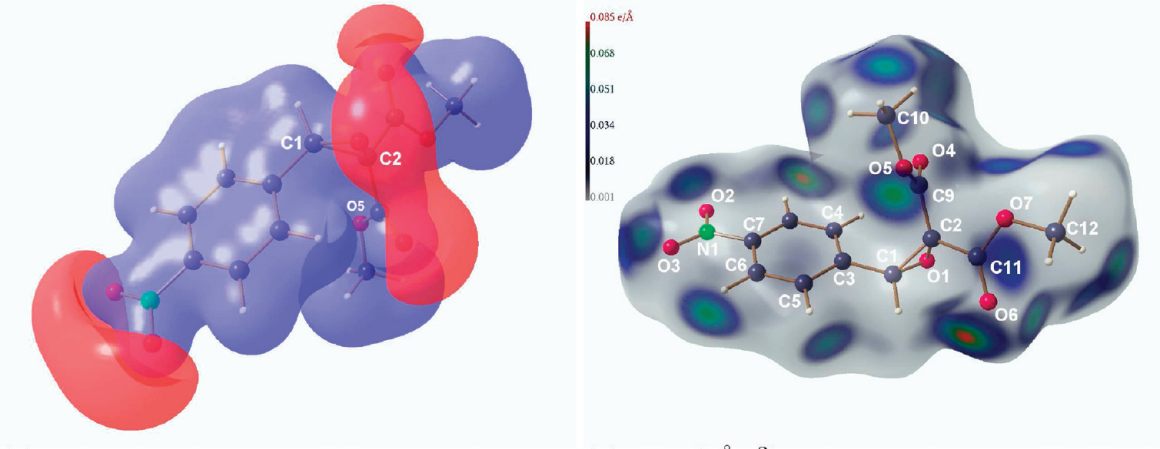

(c) ESP of cpd. **3**: Blue = isosurface of the ESP at 0.1 eÅ^{-1}, red = isosurface of the ESP at -0.1 eÅ^{-1}

(d) ED (eÅ^{-3}) mapped on a Hirshfeld surface of cpd. **3**

FIGURE 7. Representations of the experimental electrostatic potentials (ESPs) and the experimental Hirshfeld surfaces of compounds **2** and **3**.

tools to analyze the effect of different substituents were successfully tested and can be used for a rational design of molecules in various synthetic fields. Moreover, the actual impact of certain resonance formulas to the overall description of the electronic state of a molecule can be estimated by these methods. According to very recent findings, the source function is not applicable to detect resonance effects to the bcp, but only inductive effects. The source contributions of atoms as next nearest neighbors increase with the element's electronegativity, which in turn controls the amount of electron density provided by the directly bonded atoms.

A variety of intermolecular interactions was examined. N···C contacts are comparable in strength to C−H···O interactions and build a likewise stable crystal lattice. Methyl ester groups in combination with the epoxide ring form a uniform region of negative electrostatic potential, in which the main intermolecular interactions take place. This was confirmed not only by the electrostatic contributions to these interactions but also by the covalent contributions shown as electron-density code on Hirshfeld surfaces. These results may contribute to rational drug design because the active regions of these types of substituted epoxides seem to produce a recognizable and recurring pattern, which governs interactions to other molecules. This could be extrapolated to the interaction between low molecular weight ligands of this type and enzymes. Even the different degree of activity of the molecules was successfully predicted in this study by the analysis of the accumulation of interactions in the active region. However, dynamic effects and reaction rates are not accessible by X-ray diffraction on single crystals, but a more complete view of the biological activity would be possible if the cocrystallization and measurement of the epoxide-containing low molecular weight ligands inside the active pocket of the corresponding protease could be carried out. Although this is extremely difficult to realize, approaches toward this goal have recently been reported by our group[36] in that subfragments in the active region of drug−receptor complexes could be studied from a combination of X-ray data and theoretical calculations.

TABLE 3. Lattice Energies of Compounds 1−4 in kJ mol^{-1}[a]

compd	total	erd	es	es (%)
1	−51.24	−16.75	−34.49	67.3
	−50.41	−16.75	−33.66	66.8
	−46.53	−16.57	−29.95	64.4
2 molecule 1	−114.83	−36.04	−78.80	68.6
	−94.29	−38.31	−55.98	59.4
	−119.02	−36.00	−83.02	69.8
2 molecule 2	−97.76	−38.28	−59.49	60.9
	−90.48	−36.37	−54.11	59.8
	−96.82	−37.38	−59.44	61.4
3	−192.13	−89.32	−102.81	53.5
	−205.59	−92.45	−113.15	55.0
	−183.48	−88.29	−95.19	51.9
4	−101.17	−31.34	−69.83	69.0
	−128.86	−31.34	−97.51	75.7
	−102.72	−24.09	−78.64	76.6

[a]First row, experiment; second row, periodic-boundary calculations at experimental geometries; third row, periodic-boundary calculations at optimized geometries, contributions of exchange + repulsion + dispersion terms (erd, absolute) and of the electrostatic term (es, absolute and relative) to the total lattice energy.

Experimental Section

1. Synthesis and Crystallization. Commercially obtained epoxide **1** is a colorless gas at room temperature. It was crystallized in situ on a diffractometer by a method described in ref 37. For the preparation of (2*S*,3*S*)-dimethyloxirane-2,3-dicarboxylate (**2**), (*R*,*R*)-dimethyl tartrate was reacted with hydrobromic acid (HBr) in glacial acetic acid. The resulting monoacetylated tartaric acid diester was isolated and treated with HBr/acetic acid in methanol under reflux to yield (*S*,*S*)-2-bromo-3-hydroxysuccinate. Finally, potassium carbonate in acetone was added to achieve the ring closure.[38] Crystals were grown from a mixture of ethyl acetate and acetone, but the needle-shaped crystals were soft and flexible, sensitive to mechanical stress, and decomposed slowly outside their mother liquor. Quick insertion into a gas stream of cold helium or nitrogen also destroys the crystals. They could only be measured after slowly cooling down inside a vacuum chamber.

Dimethyl 3-(4-nitrophenyl)oxirane-2,2-dicarboxylate (**3**) was synthesized by the Knoevenagel condensation of malonate with *p*-nitrobenzaldehyde, followed by treatment with hypochlorite for the epoxidation.[22] Crystals were grown from a mixture of dichloromethane and methanol but tend to suffer from twinning problems. Tetracyanooxirane (**4**) was obtained from tetracyanoethylene upon reaction with hydrogen peroxide (35%) in acetonitrile.[39] Crystals of good quality were grown from a mixture of 1,2-dichloroethane and acetone.

2. Measurement and Data Processing. Details on the measurements of compounds **1**/**3** can be found in refs 21 and 22. Compound **2** was measured at the in-house Huber Eulerian four-circle diffractometer, which is equipped with a sealed Mo X-ray tube, a Bruker APEX CCD detector, a closed-cycle helium cryostat, and a transparent kapton vacuum chamber. The temperature was maintained at 25 K during the measurement. At a resolution of 1.00 Å^{-1}, the data set was complete within the face-centered monoclinic space group *C*2 (41152 measured reflections, 6618 unique). Integration of data was carried out with the program SAINT.[40] Compound **2** crystallizes enantiomerically pure (*S*,*S* configuration) with two individual molecules in the asymmetric unit and without solvent molecules. Compound **4** was measured at the synchrotron beamline F1 of HASYLAB/DESY, which is equipped with a Huber κ five-circle diffractometer, a large marCCD 165 area detector, and open-flow nitrogen gas-stream cooling. The temperature was maintained at 100 K during the measurement. At a resolution of 1.42 Å^{-1}, the data set was 99% complete within the monoclinic space group $P2_1/c$ (186756 measured reflections, 15522 unique). Integration of data was carried out with the program XDS,[41] and oblique incidence correction[42] was performed subsequently. As for compounds **1** and **3**, the asymmetric unit of compound **4** consists of one molecule, no solvent molecules are embedded in the crystal packing. Details of the measurements and data processing of all four compounds can be found in the Supporting Information.

The following data processing procedure was identical for all four compounds. The data sets were scaled and merged with the program SORTAV.[43] The structures were solved using direct methods as implemented in SHELXS.[44] Conventional spherical refinement was carried out by the program SHELXL.[44] Anisotropic displacement parameters (adps) were refined for the non-hydrogen atoms. For the hydrogen atoms, adps were calculated by a rigid-body approximation using the SHADE approach.[45] The program XDLSM of the XD2006 suite,[46] which uses the Hansen−Coppens multipole formalism[47] for aspherical modeling, was employed. A number of local symmetries and chemical constraints were used; for details see the Supporting Information. All non-hydrogen atoms were treated up to the hexadecapole level of expansion, whereas monopoles, bond-directed dipoles, and bond-directed quadrupoles were introduced for hydrogen atoms. The expansion−contraction parameter κ was refined independently for all chemically nonsimilar non-hydrogen atoms. κ′ values were left at their default values κ′ = 1.0, but for hydrogen atoms, optimized values κ = 1.13 and κ′ = 1.29[48] were used. All bond distances involving hydrogen atoms were fixed to mean neutron diffraction values from the literature.[49] H−C−H bond angles in methyl groups were fixed to the tetrahedral angle. An electroneutrality constraint concerning the monopole populations was applied for the asymmetric units. For compound **2**, starting multipoles had to be determined from theoretical structure factors (program CRYSTAL06[50]) to ensure a stable refinement. Deformation densities, Laplacian densities, the source function, electrostatic potentials, interaction and lattice energies, atomic properties, Hirshfeld surfaces, as well as the ED and Laplacian values at the bcps were determined with the program XDPROP of the XD2006 suite. Graphical representations of deformation density and Laplacian were done with XDGRAPH. The program DIAMOND[51] was used for graphics involving the source function. Isosurface representations (electrostatic potentials and Hirshfeld surfaces) were produced using the program MOLISO.[52]

(37) Luger, P.; Buschmann, J. *J. Am. Chem. Soc.* **1984**, *106*, 7118.
(38) Miller, M. W. *J. Med. Chem.* **1963**, *6*, 233.
(39) Linn, W. J.; Webster, O. W.; Benson, R. E. *J. Am. Chem. Soc.* **1965**, *87*, 3651.
(40) Bruker AXS Inc., Madison, WI, *SMART and SAINT Data Collection and Processing Software for the SMART System*, 1995−2005.
(41) Kabsch, W. *J. Appl. Crystallogr.* **1988**, *21*, 916.
(42) Johnas, S. K. J.; Morgenroth, W.; Weckert, E. *HASYLAB Annual Report* **2006**, 325.
(43) Blessing, R. H.; Langs, D. A. *J. Appl. Crystallogr.* **1987**, *20*, 427.
(44) Sheldrick, G. M. *Acta Crystallogr. A* **2008**, *64*, 112.
(45) Madsen, A. Ø.; Sørensen, H. O.; Flensburg, C.; Stewart, R. F.; Larsen, S. *Acta Crystallogr. A* **2004**, *60*, 550.
(46) Volkov, A.; Macchi, P.; Farrugia, L. J.; Gatti, C.; Mallinson, P. R.; Richter, T.; Koritsánszky, T. S. *XD2006 - a Computer Program for Multipole Refinement, Topological Analysis and Evaluation of Intermolecular Energies from Experimental and Theoretical Structure Factors*, **2006**.
(47) Hansen, N. K.; Coppens, P. *Acta Crystallogr. A* **1978**, *34*, 909.
(48) Volkov, A.; Abramov, Y.; Coppens, P. *Acta Crystallogr. A* **2001**, *57*, 272.
(49) Allen, F. H.; Kennard, O.; Watson, D. G.; Brammer, L.; Orpen, A. G.; Taylor, R. *International Tables for X-ray Crystallography*; Kluwer Academic Publishers: Amsterdam, 1992; Vol. C, Chapter 9.5, p 685.
(50) Dovesi, R.; Saunders, V. R.; Roetti, C.; Orlando, R.; Zicovich-Wilson, C. M.; Pascale, F.; Civalleri, B.; Doll, K.; Harrison, N.; Bush, I.; DArco, P.; Llunell, M. *CRYSTAL06, version 1.0.2*, **2008**.
(51) Bergerhoff, G.; Berndt, M.; Brandenburg, K. *J. Res. Natl. Inst. Stand. Technol.* **1996**, *101*, 221.

3. Theoretical Calculations. Isolated-molecule calculations were performed for compounds **1**−**4** with the program GAUSSIAN03[53] at experimental geometries after multipole refinement and at optimized geometries. The B3LYP/cc-pVTZ level of theory was used. Topological analysis of the ED was performed with AIM2000.[54]

The experimental geometries of compounds **1**−**4** were used as input for periodic-boundary calculations with the program CRYSTAL06[50] (levels of theory: 6-311G(d) for O, N, and C,[55] 3−11G(p) for H[55]). Not only calculations at fixed experimental geometry but also geometry optimizations within the crystal environment were performed. The space group was fixed, but lattice constants as well as bond distances and angles were optimized. From the periodic wave function for both experimental and optimized geometries, static theoretical structure factors were calculated with the program PROPERTIES06 of the CRYSTAL06 suite of programs. The same list of *hkl* indices as measured was chosen to be calculated. Within a modeling of the theoretical structure factors with XD2006, the same density models were used as for experimental structure factors. Results were produced with the program XDPROP. Details of the final optimized crystal geometries and details of the refinements of theoretical structure factors are given in the Supporting Information.

Acknowledgment. We acknowledge the DFG (Deutsche Forschungsgemeinschaft) for financial support of this project within the special priority program SPP1178. We also thank Dr. Stefan Mebs, Dr. Roman Kalinowski, and Dipl.-Chem. Julian Holstein for their help during the high-resolution measurements.

Supporting Information Available: CIF files of compounds **1**−**4** (CIF files CCDC-691554, 776785, 675061, and 776784 can also be obtained free of charge from the Cambridge Crystallographic Data Centre via www.ccdc.cam.ac.uk/data_request/cif); crystallographic and refinements details; multipole refinement strategies and κ/κ' values; residual density maps; details of refinements on theoretical structure factors; three-dimensional isosurface representations of the static deformation density and the Laplacian of the epoxide ring and the ester groups; two-dimensional static deformation−density maps in the methyl ester and nitrophenyl groups; complete lists of bond-topological and atomic properties; representations of bond-topological and atomic properties of bonds to substituents or atoms in substituents that are directly bonded to the epoxide rings; absolute values of the source function; representations of the relative atomic contributions to C−O bonds in the epoxide rings from the source function; complete hydrogen-bonding patterns. This material is available free of charge via the Internet at http://pubs.acs.org.

(52) Hübschle, C. B.; Luger, P. *J. Appl. Crystallogr.* **2006**, *39*, 901.
(53) Frisch, M. J. et al. *Gaussian 03, revision E.01*; Gaussian, Inc., Wallington CT, 2004.
(54) Biegler-König, F.; Schönbohm, J.; Bayles, D. *J. Comput. Chem.* **2001**, *22*, 545.
(55) Gatti, C.; Saunders, V. R.; Roetti, C. *J. Chem. Phys.* **1994**, *101*, 10686.